Strong Atom-Cavity Coupling over Large Volumes and the Observation of Subnatural Intracavity Atomic Linewidths

S. E. Morin, C. C. Yu, and T. W. Mossberg
Department of Physics, University of Oregon, Eugene, Oregon 97403
(Received 11 October 1993)

Standard classical optical design procedures along with the intuitive concept of hour-glass-type optical modes are employed to produce cavities that provide strong atom-cavity coupling for atoms spread over a relatively large spatial region. Such cavities may be employed to provide macroscopic environments in which ordinarily microscopic quantum optical phenomena play an essential role. Concepts are tested through explicit cavity fabrication combined with an experimental study of cavity-mediated perturbations to the frequency and width of a spontaneous emission line in atomic barium. Manifestly subnatural emission linewidths are observed.

PACS numbers: 42.50.−p, 32.70.Jz, 42.15.Eq, 42.60.Da

Cavity quantum electrodynamics (cavity QED) may be loosely described as the study of atom-field dynamics in the presence of boundaries [1–4]. Boundaries (collectively constituting a "cavity") are significant in that they perturb the spatial and/or spectral structure and distribution of electromagnetic field modes relative to the free-space norm, thereby opening the door to new and unique phenomenology. A wide range of physical systems fall within the scope of cavity QED. At one extreme, we have an isolated atom interacting with a single undamped field mode [5]. More realistically, systems may consist of atoms and field modes all of which experience damping due to the interaction with one or more reservoirs. Many physical models have been considered and numerous categories of cavity QED phenomena have been identified [6–18].

Phenomena that are specifically identified with cavity QED tend to appear in the regime of strong *atom-cavity coupling*, i.e., when the interaction of an atom with a single cavity photon becomes important. In theoretical modeling, one has only to adjust the relevant parameters to reach this regime. Physical realization of strong atom-cavity coupling is more difficult. For the most part, experimenters have worked with one basic cavity parameter in their efforts to realize strong atom-cavity coupling, the overall cavity mode volume. Through minimization of this parameter, relatively strong atom-cavity coupling has been realized in both the optical [4,10,17] and microwave regimes [7,14]. Cavity mode volume does not, however, tell the whole story. Strong atom-cavity coupling has, for example, been demonstrated in large (centimeter-scale) optical cavities [15,16], and attributed to the combined effect of many spectrally degenerate large-volume modes. In this Letter, we analyze *atom-cavity coupling* from an alternative perspective based on mode geometry [3], and show how classical optical design methods can be employed to create macroscopic environments wherein normally microscopic quantum optical phenomena play an essential role.

The modes of optical cavities are frequently discussed in terms of relatively low order Hermite-Gaussian functions [19]. While vital from the perspective of laser operation and other applications, these paraxial modes generally do not serve to optimize atom-cavity coupling. An entirely different type of mode, one rarely considered in the context of quantum optics, is shown in Fig. 1. An hour-glass-shaped mode has extreme spatial inhomogeneity. In some regions, the mode exhibits very tight focusing and hence strong atom-cavity coupling while in other regions the mode has a large diameter and concomitant weak atom-cavity coupling. Provided that the f number $f/D \approx 1$, where $f(D)$ is the focal length (beam diameter) as shown in Fig. 1, the spot size w at the mode waists can be comparable to the field wavelength λ.

The strength of an atom's coupling to a field mode is conveniently expressed in terms of g, the atom's single-photon Rabi frequency. Incorporating all mode-independent factors into a constant α_a, we write $g = \alpha_a E_m$, where E_m is the magnitude of the modal electric field at the atom's location when the mode is occupied by a single photon. The value of E_m at the waist of an hour-glass mode (in a λ-scale-cavity mode) is proportional to $1/w\ell^{1/2}$ $(1/\lambda^{3/2})$, where ℓ is the path length of the hour-glass mode. The g factors of hour-glass ($w \approx \lambda$) modes and λ-scale-cavity modes differ only by a factor on the order of $(\lambda/\ell)^{1/2}$. We note that the cavity quality factor (Q) does not enter into determining g.

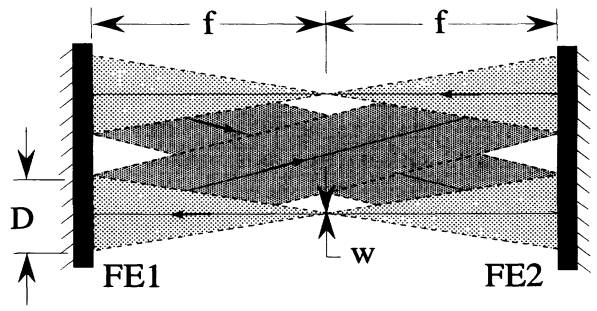

FIG. 1. An hour-glass mode. FE denotes a focusing element.

0031-9007/94/73(11)/1489(4)$06.00

At first thought, one might conclude that large g factors and large cavity volumes are inconsistent. Actually, optical design techniques can be applied to create cavities that support a multitude of hour-glass modes (collectively forming a *composite* mode), whose waists collectively span a volume much larger than the focal volume of a single hour-glass mode. Importantly, the cavity field within the active volume of a composite-mode cavity possesses complexity not found in a single-mode field. The fields associated with individual hour-glass modes are generally incoherent. Thus, an atom traveling through the active volume of a composite mode will see random phase changes as it passes individual hour-glass modes. These phase changes can be safely ignored, however, if the modal field coherence time associated with individual hour-glass modes, τ_c, is significantly shorter than the atomic transit time across individual hour-glass modes. On the other hand, collective atomic effects that may occur when many atoms reside in a single-mode cavity will generally be suppressed in a composite-mode cavity, since atoms within constituant hour-glass modes will not be able to communicate effectively. We conclude that as long as only single-atom effects are important and τ_c is sufficiently short, a moving atom can be treated as if it were interacting with a single hour-glass mode as it travels through the active volume of a composite-mode cavity.

The problem of designing a large g-factor cavity supporting a large-active-volume composite mode can restated as a classical optical design problem as follows: The cavity end reflectors (focusing elements) must provide diffraction-limited, f number $\cong 1$ imaging of rays originating from any point inside the cavity's active volume back onto their source point (self-imaging) after passing through the cavity one or more times. Degeneracy is ensured by demanding constancy of source-to-image optical path length throughout the cavity's active volume. Optimization works toward minimizing the working f number of the focusing elements and maximizing the active volume of the cavity. The use of multielement lens reflectors in place of the bare mirrors normally employed in cavity design [15,16,19,20] allows considerable flexibility in realizing a cavity having a large g factor and a large active volume simultaneously.

We have constructed a confocal *optical* cavity [21] that supports multiple λ-scale waist hour-glass modes over a large active volume and tested its quantum optical properties. The cavity is comprised of two coaxial lens reflectors each consisting of a doublet lens whose external convex surface has a reflective dielectric coating [see Fig. 2(a)]. Off-axis (on-axis) source points couple to modes resembling those shown in Fig. 1 [Fig. 2(b)]. Diffraction-limited, f number of 1 self-imaging is achieved over an active region 200 μm in diameter. The effective focal length (working aperture diameter) of the lens reflector is $f = 10$ mm ($D = 10$ mm). The cavity free-spectral range is $\Delta\nu_{\rm fsr} = c/4\ell = 2.6$ GHz, where $\ell = 28.6$ mm is the end-to-end optical path length at $\lambda = 553$ nm and c is

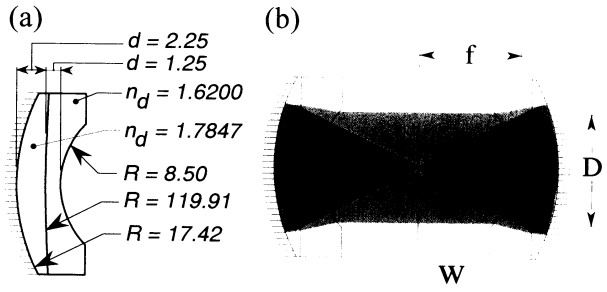

FIG. 2. (a) Diffraction-limited, large-solid-angle (f number of 1) lens reflector employed to maximize g. Dimensions are in mm. (b) Lens-reflector confocal optical cavity assembly: $f = D = 10.0$ mm; $w \cong \lambda$.

the speed of light. Anticipating the need to couple atomic beam fluorescence with large Doppler shifts into the large-solid-angle cavity mode, a low reflectivity dielectric coating ($R = 0.85$) was applied to the external convex surface ensuring a sufficiently broad cavity resonance. At full working aperture, the full width at half maximum (FWHM) of the cavity resonance was measured to be $\Delta\nu_{\rm mode} = 540$ MHz giving a finesse of $\mathcal{F} = 4.8$ and implying a cavity coherence time $\tau_c = 1/2\pi\Delta\nu_{\rm mode} \approx 300$ psec.

A well known cavity QED effect is the modification of atomic spontaneous emission [1–4,8–10,13–18]. The largeness of our cavity bandwidth relative to g leads us to expect atoms within the active volume of our cavity to display exponential spontaneous atomic decay with a rate that can be written as

$$\gamma_s = \gamma_{\rm cav}(\Delta) + \gamma_{\rm back}\,, \tag{1}$$

where $\gamma_{\rm cav}$ ($\gamma_{\rm back}$) represents decay associated with the cavity mode (open sides of the cavity) and $\Delta \equiv \nu_{\rm atom} - \nu_{\rm cav}$, where $\nu_{\rm atom}$ ($\nu_{\rm cav}$) is the atomic (cavity) resonance frequency. The functional form of $\gamma_{\rm cav}(\Delta)$ depends on the detailed resonance properties of the cavity. In the case of atom-cavity resonance and assuming $\gamma_{\rm cav}\tau_c \ll 1$, we can write [3]

$$\gamma_{\rm cav}(0) = \frac{2}{\pi}\left(\frac{D}{\ell}\right)^2 \mathcal{F}\gamma_{\rm fs}\,, \tag{2a}$$

where $\gamma_{\rm fs}$ is the free-space Einstein A coefficient. We also have [9]

$$\frac{g^2}{\pi\Delta\nu_{\rm mode}} = \frac{\gamma_{\rm cav}}{2}\,. \tag{2b}$$

As the atom-cavity detuning is increased $\gamma_{\rm cav} \to 0$. Thus, by measuring γ_s with the cavity tuned on and off resonance we can deduce g. Applying Eq. (2) to our cavity, we expect $\gamma_{\rm cav}(0) \cong 0.37\gamma_{\rm fs}$ and $g \cong 1.6\gamma_{\rm fs}$.

To test the quantum optical properties of our cavity, a Ba atomic beam (diameter ≈ 120 μm, residual transverse Doppler width ≈ 1 MHz) of natural isotopic composition is directed through the active volume of the cavity where it intersects the waist of a focused Gaussian $\rm TEM_{00}$ laser beam (laser beam waist ≈ 120 μm). The cavity axis, the

atomic beam, and the laser beam are mutually orthogonal (see Fig. 3). The laser beam is generated by a single-longitudinal-mode, ring-dye-laser system. The dye-laser frequency is locked (via a saturation spectroscopy laser-locking scheme [22]) to the 553.5 nm transition ($6s^2\,{}^1S_0$-$6s6p\,{}^1P_1$) of ^{138}Ba in an auxiliary vapor cell. The frequency of the locked laser is scanned across an 80 MHz range using a voltage-controlled-oscillator (VCO) driven acousto-optic modulator (AOM). The AOM is double passed to provide deflection-free tuning. A fraction of the VCO output is sent to a computer-monitored frequency counter. The laser frequency is stepped across the atomic transition while the atomic fluorescence intensity emitted out one end of the cavity is recorded. Fluorescence emitted by atoms within a region approximately 100 μm across was collected. Owing to the low finesse of the cavity, spectral filtering of the atomic fluorescence can be neglected. The resulting weak-field absorption spectra are fit by a Lorentzian function with adjustable height, width, center frequency, and background. Note that τ_c is approximately an order of magnitude shorter than the single-hour-glass-mode transit time in our apparatus. We therefore expect Eq. (2) to be valid and can ignore the composite-mode nature of our cavity's active volume.

In Fig. 4(a), we present measured atomic absorption linewidths (FWHM) for two different cavity tunings. The open circles (open triangles) show the absorption linewidth with the cavity tuned to maximize (minimize) the atomic fluorescence intensity into the cavity mode; i.e., the cavity is tuned into (out of) resonance with the atom and $\Delta = 0$ ($\Delta \approx \Delta\nu_{\rm fsr}/2$). The only experimental parameter changing from data set to data set is the voltage applied to the piezoelectric transducer (PZT) which adjusts the cavity length and thus the resonance frequency of the cavity. Each data set shows five independent measurements of the linewidth at the chosen cavity length.

The lifetime of the $6s6p\,{}^1P_1$ level in Ba is 8.37 ± 0.08 nsec [23]. The Fourier-transform radiative linewidth

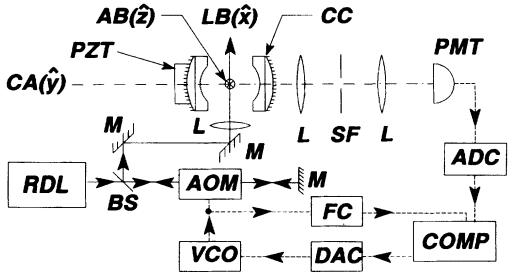

FIG. 3. Experimental apparatus: RDL, externally stabilized ring dye laser; L, lens; SF, spatial filter; M, mirror; BS, beam splitter; AOM, acousto-optic modulator; VCO, voltage-controlled oscillator; FC, frequency counter; DAC, digital-to-analog converter; ADC, analog-to-digital converter; COMP, IBM AT with GPIB and CAMAC interfaces; PMT, photomultiplier tube; CC, confocal optical cavity; CA, cavity axis; AB, atomic beam (into page); LB, laser beam; PZT, piezoelectric transducer.

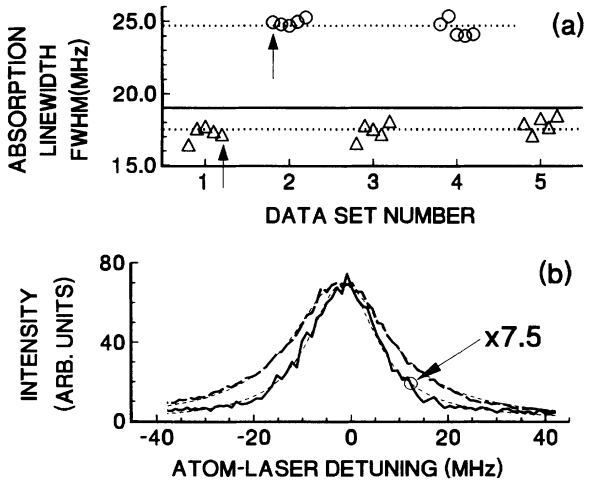

FIG. 4. (a) Cavity-modified atomic radiative linewidth (FWHM). Circles (triangles) indicate FWHM for $\Delta = 0$ ($\Delta \sim \Delta\nu_{\rm fsr}/2$) where $\Delta = \nu_{\rm atom} - \nu_{\rm cav}$. The solid line indicates the free-space radiative linewidth [23]. (b) Two weak-field absorption spectra from Fig. 4(a) (marked with arrows). The solid (dashed) line spectrum was taken with $\Delta \sim \Delta\nu_{\rm fsr}/2$ ($\Delta = 0$) where FWHM = 17.1 MHz (24.9 MHz). The solid line spectrum intensity was multiplied by 7.5 for plotting. The thin dashed lines are fitted Lorentzians.

is therefore 19.0 ± 0.2 MHz. The supernatural absorption linewidth of 24.7 ± 0.2 MHz observed when the atom and cavity were resonant indicates a cavity-mediated enhancement of the spontaneous emission rate. The 17.5 ± 0.2 MHz linewidth observed when $\Delta \approx \Delta\nu_{\rm fsr}/2$ explicitly demonstrates a cavity-mediated inhibition of spontaneous emission. To our knowledge, this is the first observation of a cavity-mediated, manifestly subnatural atomic linewidth. In Ref. [15], manifestly subnatural linewidths were masked by the effects of transit time across the small active volume of the cavity employed. In our mode geometry point of view, the cavity of Ref. [15] can be described as supporting a single hour-glass mode. In Fig. 4(b), we show two representative spectra from Fig. 4(a). The measurements of Fig. 4(a) indicate that $\gamma_{\rm cav}(0) = 0.38\gamma_{\rm fs}$ which is consistent with our estimate based on the cavity parameters and Eq. (2a). Using Eq. (2b), our measured g factor is $1.6\gamma_{\rm fs}$.

We have also observed cavity-mediated shifts [2,15,24] in the atomic emission frequency. We define the shift as

$$\delta\nu_{\rm atom}(\Delta) \equiv \nu_{\rm atom}(\Delta) - \nu_{\rm atom}(0), \qquad (3)$$

where $\nu_{\rm atom}(\Delta)$ is the center frequency of the atomic absorption spectrum measured with an atom-cavity detuning Δ. In making the shift measurements, the cavity frequency was not measured directly. Rather, the cavity was tuned to the red or blue of the atomic transition until the peak atomic fluorescence intensity into the cavity mode fell to one-half of its maximum, i.e., $\Delta = 0$ value. A shift of -0.41 ± 0.02 MHz ($+0.95$ ± 0.02 MHz) was observed

when the cavity was tuned to the red (blue). Inasmuch as the shift is related to the detailed shape of the cavity spectral response function [2], we attribute the observed spectral asymmetries in the former quantity to a similar asymmetry observed in the latter. The shift magnitude observed is consistent with a value calculated using our known g value together with the assumption that the shift arises from a vacuum-field dressing of the atomic states.

In conclusion, we have demonstrated that strongly focused hour-glass modes provide for strong atom-cavity coupling even in the case of centimeter-scale optical cavities. We have shown, by experimental demonstration, that classical optical design techniques can be applied to create cavities supporting a multitude of λ-scale-waist hour-glass modes, collectively spanning an active volume dramatically larger than that characteristic of a single-hour-glass mode. By identifying the classical mode properties necessary for the realization of strong atom-cavity coupling, one converts a quantum optical design problem into an entirely classical one. Our experiments indicate that we have in fact realized a strong atom-cavity coupling over a large volume. This fact has allowed us to measure, for the first time, a manifestly subnatural radiative linewidth in a cavity-confined atomic system.

We gratefully acknowledge support from the National Science Foundation, Grant No. PHY91-03132, and the Army Research Office, Grant No. DAAL03-91-G-0313.

[1] Serge Haroche and Daniel Kleppner, Phys. Today **42**, No. 1, 24 (1989); P. Meystre, in *Nonlinear Optics in Solids*, edited by O. Keller (Springer-Verlag, Berlin, 1990), p. 26; S. Haroche, in *Fundamental Systems in Quantum Optics*, edited by J. Dalibard, J.-M. Raimond, and J. Zinn-Justin (North-Holland, Amsterdam, 1992), p. 767; P. Meystre, in *Progress in Optics*, edited by E. Wolf (North-Holland, Amsterdam, 1992), Vol. 30, p. 261; *Development and Applications of Materials Exhibiting Photonic Band Gaps*, edited by C. M. Bowden, J. P. Dowling, and H. O. Everitt [J. Opt. Soc. Am. B **10**, 279 (1993)].

[2] E. A. Hinds, Adv. At. Mol. Opt. Phys. **28**, 237 (1991).

[3] S. E. Morin, Q. Wu, and T. W. Mossberg, Opt. Photon. News **3**, 8 (1992); T. W. Mossberg and M. Lewenstein, Adv. At. Mol. Opt. Phys. Suppl. **2**, 171 (1994).

[4] Y. Yamamoto and R. Slusher, Phys. Today **46**, No. 6, 66 (1993).

[5] E. T. Jaynes and F. W. Cummings, Proc. IEEE **51**, 89 (1963).

[6] J. H. Eberly, N. B. Narozhny, and J. J. Sanchez-Mondragon, Phys. Rev. Lett. **44**, 1323 (1980); N. Nayak, R. K. Bullough, B. V. Thompson, and G. S. Agarwal, IEEE J. Quantum Electron. **24**, 1331 (1988); S. M. Barnett and P. L. Knight, Phys. Rev. A **33**, 2444 (1986).

[7] G. Rempe, H. Walther, and N. Klein, Phys. Rev. Lett. **58**, 353 (1987).

[8] J. J. Sanchez-Mondragon, N. B. Narozhny, and J. H. Eberly, Phys. Rev. Lett. **51**, 550 (1983); G. S. Agarwal, Phys. Rev. Lett. **53**, 1732 (1984); Y. Zhu, D. J. Gauthier, S. E. Morin, Qilin Wu, H. J. Carmichael, and T. W. Mossberg, Phys. Rev. Lett. **64**, 2499 (1990); F. Bernardot, P. Nussenzveig, M. Brune, J. M. Raimond, and S. Haroche, Europhys. Lett. **17**, 33 (1992).

[9] H. J. Carmichael, R. J. Brecha, M. G. Raizen, H. J. Kimble, and P. R. Rice, Phys. Rev. A **40**, 5516 (1989).

[10] R. J. Thompson, G. Rempe, and H. J. Kimble, Phys. Rev. Lett. **68**, 1132 (1992).

[11] H. J. Carmichael, Phys. Rev. Lett. **55**, 2790 (1985); P. L. Knight and T. Quang, Phys. Rev. A **41**, 6255 (1990).

[12] C. M. Savage, J. Mod. Opt. **37**, 1711 (1990); P. Alsing, D.-S. Guo, and H. J. Carmichael, Phys. Rev. A **45**, 5135 (1992).

[13] E. M. Purcell, Phys. Rev. **69**, 681 (1946); K. H. Drexhage, in *Progress in Optics*, edited by E. Wolf (North-Holland, Amsterdam, 1974), Vol. 12, p. 163; D. Kleppner, Phys. Rev. Lett. **47**, 233 (1981); R. G. Hulet, E. S. Hilfer, and D. Kleppner, Phys. Rev. Lett. **55**, 2137 (1985); F. De Martini, G. Innocenti, G. R. Jacobovitz, and P. Mataloni, Phys. Rev. Lett. **59**, 2955 (1987); W. Jhe, A. Anderson, E. A. Hinds, D. Meschede, L. Moi, and S. Haroche, Phys. Rev. Lett. **58**, 666 (1987); E. Yablonovitch, T. J. Gmitter, R. D. Meade, A. M. Rappe, K. D. Brommer, and J. D. Joannopoulos, Phys. Rev. Lett. **67**, 3380 (1991); S. John and J. Wang, Phys. Rev. Lett. **64**, 2418 (1990); H. Chew, Phys. Rev. A **38**, 3410 (1988).

[14] P. Goy, J. M. Raimond, M. Gross, and S. Haroche, Phys. Rev. Lett. **50**, 1903 (1983).

[15] D. J. Heinzen and M. S. Feld, Phys. Rev. Lett. **59**, 2623 (1987).

[16] D. J. Heinzen, J. J. Childs, J. E. Thomas, and M. S. Feld, Phys. Rev. Lett. **58**, 1320 (1987); Y. Zhu, A. Lezama, T. W. Mossberg, and M. Lewenstein, Phys. Rev. Lett. **61**, 1946 (1988); A. Lezama, Y. Zhu, S. Morin, and T. W. Mossberg, Phys. Rev. A **39**, 2754 (1989).

[17] A. M. Vredenberg, N. E. J. Hunt, E. F. Schubert, D. C. Jacobson, J. M. Poate, and G. J. Zydzik, Phys. Rev. Lett. **71**, 517 (1993).

[18] M. Lewenstein and T. W. Mossberg, Phys. Rev. A **37**, 2048 (1988).

[19] A. E. Siegman, *Lasers* (University Science Books, Mill Valley, CA, 1986).

[20] M. Hercher, Appl. Opt. **7**, 951 (1968).

[21] The confocal optical cavity was designed according to our specifications by Optical Research Associates of Pasadena, CA and fabricated by TORC of Tucson, AZ.

[22] R. W. P. Drever, J. L. Hall, F. V. Kowalski, J. Hough, G. M. Ford, A. J. Munley, and H. Ward, Appl. Phys. B **31**, 97 (1983).

[23] F. M. Kelley and M. S. Mathur, Can. J. Phys. **55**, 83 (1977).

[24] P. Dobiasch and H. Walther, Ann. Phys. (Paris) **10**, 825 (1985); E. A. Hinds and V. Sandoghdar, Phys. Rev. A **43**, 398 (1991); C. I. Sukenik, M. G. Boshier, D. Cho, V. Sandoghdar, and E. A. Hinds, Phys. Rev. Lett. **70**, 560 (1993).

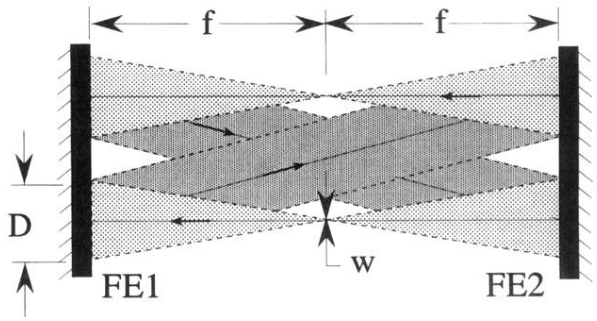

FIG. 1. An hour-glass mode. FE denotes a focusing element.

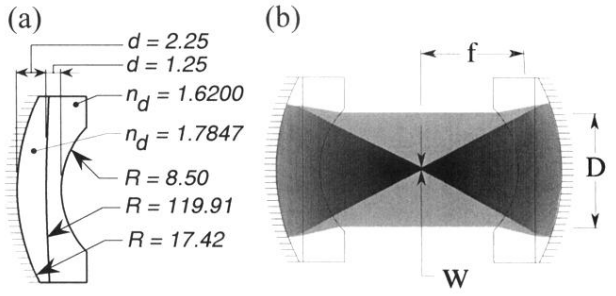

FIG. 2. (a) Diffraction-limited, large-solid-angle (f number of 1) lens reflector employed to maximize g. Dimensions are in mm. (b) Lens-reflector confocal optical cavity assembly: $f = D = 10.0$ mm; $w \cong \lambda$.